Mobius3D

THE COMPLETE PATIENT QA SYSTEM

- **3D PATIENT PLAN QA**
- **3D IMRT/VMAT PRE TREATMENT QA**
- **3D *IN VIVO* DAILY TREATMENT QA**
- **ONLINE PATIENT POSITIONING QA**

Upgrade your patient safety by bridging the gap between patient QA and machine QA:

DoseLab, the complete TG-142 solution, is now integrated into Mobius3D!

Visit mobiusmed.com/mobius3d to learn more or register for a bi-weekly webinar at mobiusmed.com/webinars

MOBIUS MEDICAL SYSTEMS
INNOVATIVE SOFTWARE FOR MODERN RADIATION ONCOLOGY

Received Date: 13-Apr-2016

Revised Date: 13-Jan-2017

Accepted Date: 03-Feb-2017

Article Type: Research Article

Image noise and dose performance across a clinical population: patient size adaptation as a metric of CT performance

Francesco Ria[a)]

Carl E. Ravin Advanced Imaging Labs and Clinical Imaging Physics Group, Duke University Health System, Durham NC 27705; Dipartimento Diagnostica per Immagini, Centro Diagnostico Italiano, Milan ITALY; Alumnus progettoDiventerò di Fondazione Bracco, Milan ITALY

Joshua Mark Wilson

Clinical Imaging Physics Group, Duke University Health System, Durham NC 27705

Yakun Zhang

Carl E. Ravin Advanced Imaging Labs and Clinical Imaging Physics Group, Duke University Health System, Durham NC 27705

This article has been accepted for publication and undergone full peer review but has not been through the copyediting, typesetting, pagination and proofreading process, which may lead to differences between this version and the Version of Record. Please cite this article as doi: 10.1002/mp.12172

Ehsan Samei

Carl E. Ravin Advanced Imaging Labs and Clinical Imaging Physics Group, Duke University Health System, Durham NC 27705

PURPOSE. Modern CT systems adjust x-ray flux accommodating for patient size to achieve certain image noise values. The effectiveness of this adaptation is an important aspect of CT performance and should ideally be characterized in the context of real patient cases. The objective of this study was to characterize CT performance with a new metric that includes image noise and radiation dose across a clinical patient population.

MATERIALS AND METHODS. The study included 1526 examinations performed by three CT scanners (one GE Healthcare Discovery CT750HD, one GE Healthcare Lightspeed VCT, and one Siemens SOMATOM definition Flash) used for two routine clinical protocols (abdominopelvic with contrast and chest without contrast). An institutional monitoring system recorded all the data involved in the study. The dose-patient size and noise-patient size dependencies were linearized by considering a first order approximation of analytical models that describe the relationship between ionization dose and patient size, as well as image noise and patient size. A 3D-fit was performed for each protocol and each scanner with a planar function, and the Root Mean Square Error (RMSE) values were estimated as a metric of CT adaptability across the patient population.

RESULTS. The data show different scanner dependencies in terms of adaptability: the RMSE values for the three scanners are between 0.0385 $HU^{1/2}$ and 0.0215 $HU^{1/2}$.

CONCLUSIONS. A theoretical relationship between image noise, $CTDI_{vol}$ and patient size was determined based on real patient data. This relationship may be interpreted as a new metric related to the scanners' adaptability concerning image quality and radiation dose across a patient population. This method could

be implemented to investigate the adaptability related to other image quality indexes and radiation dose in a clinical population.

Key words: image noise, radiation dose, patient population, CT performance

1. INTRODUCTION

CT diagnostic protocols should be designed and optimized to balance image quality and radiation dose and clinically acceptable image quality has become an issue as dose reduction strategies. The aim of optimization must be to keep radiation exposure "as low as reasonably achievable" (ALARA) while ensuring acceptable clinical images [1-2]. Therefore, behind every optimization action, there is need of a risk/benefit evaluation. The effort to contextually compare the image quality and radiation dose is a natural progression of the optimization principle [2] because the acquisition parameters are directly related to the clinical benefit: dose is correlated with patient risk. The balance between risk and benefit for a given exam is governed by the adaptation mechanisms implemented in modern CT.

CT devices are designed with the capability to modulate the radiation output that is administered to achieve consistency in image quality across patients. For example, automatic tube current modulation systems (ATCM) control the tube current according to the anatomical size and body habitus [3-6]. But, how does this adaptability extend to a real patient population with diverse attributes? There is a need to evaluate the performance of adaptation in the context of optimization across a patient population because a phantom study may only provide information related to the scanner performance in a highly-constrained setup [7].

The work shown here measures CT performance with a new metric that simultaneously incorporates image noise and radiation dose across a patient population. The aim was to quantify how CT scanners balance image quality and radiation dose, by adjusting exposure parameters, as a function of patient size. This methodology can be implemented within dose monitoring programs that collect patient size, dose, and image noise values [8], which allows CT performance characterization across patient populations.

2. MATERIAL AND METHODS

This study has been performed in compliance with HIPAA and IRB guidelines. Three scanners are involved in the study: one GE Healthcare Discovery CT750HD, one GE Healthcare Lightspeed VCT and one Siemens Healthcare SOMATOM Definition Flash.

2.A. Imaging cases

This study included 1526 examinations (January 2015 and June 2015 through January 2016) performed by three CT and two clinical protocols: abdominopelvic with contrast (A&P w) and chest without contrast (Chest wo) as reported in Tables 1 and 2 and Figure 1. In order to consider only the diagnostic series, scout, iterative reconstruction, contrast monitoring, and contrast pre-monitoring series were excluded. The patient size populations were qualitatively evaluated to ensure that there were not unexpected size trends in the samples: a normal distribution indicates that there are not excesses in small or obese patients (Fig. 2).

Since the proposed method needs to be applied to consistent populations in term of scan parameters and convolution kernels, for each protocol, we selected the most frequent exams with the same kVp, slice thickness, total collimation width, pitch, convolution kernel, and image quality indicator. GE

Healthcare and Siemens Healthcare scanners use two distinct angular ATCM methodologies with target image quality indicators corresponding to varying degrees of image quality. The image quality indicators are noise index (NI) for GE Healthcare and image quality reference effective tube current-time product (Q) for Siemens Healthcare scanners. In this work, we included the corresponding level of image quality index for each protocol. In the further sections, the three scanners are identified as CT1, CT2 and CT3.

Table 1. Summary of examinations included in the study sorted by scanners, clinical protocol, and scan parameters. NI (noise index) is the image quality indicator for GE Healthcare scanners and Q (image quality reference effective tube current-time product) is the image quality indicator for Siemens Healthcare scanners.

Protocol	CT scanners	Number of patients	Slice thickness (mm)	Total collimation width (mm)	Convolution kernel	kVp	Pitch	NI-Q
A&P w	GE Discovery CT750HD	266	0.625	40	Standard	120	1.375	220
	GE Lightspeed VCT	407	5	40	Standard	120	1.375	150
	SIEMENS SOMATOM Definition Flash	323	0.6	38.4	I31F	120	0.8	200
Chest wo	GE Discovery CT750HD	414	5	40	Standard	120	1.375	160
	GE Lightspeed VCT	48	5	40	Standard	120	1.375	160
	SIEMENS SOMATOM Definition Flash	68	5	38.4	B31F	120	0.8	150

Table 2. Summary of the patient population demographics in this study per devices and protocols.

Code	Patient age (years) (range, mean, median)	Patient effective diameter (cm) (range, mean, median)	Noise value (HU) (range, mean, median)	$CTDI_{vol}$ (mGy) (range, mean, median)
CT1 A&P w	[14.0, 90.0]; 53.4; 55.5	[21.0,41.7]; 29.9; 29.9	[19.0, 42.5]; 29.6; 29.1	[3.9, 21.5]; 9.3; 7.9
CT1 Chest wo	[17.0, 94.0]; 62.1; 65.0	[24.0, 40.7]; 32.9; 33.0	[9.6, 23.9]; 12.6; 12.4	[2.4, 38.2]; 9.9; 9.9
CT2 A&P w	[15.0, 97.0]; 51.5; 50.0	[20.7, 42.2]; 29.7; 29.4	[9.1, 34.6]; 17.4; 17.1	[2.7, 30.4] 12.0, 11.4

CT2 Chest wo	[13.0, 89.0]; 63.3; 64.0	[25.8, 37.6]; 31.7; 31.5	[13.9, 23.5]; 18.1; 17.9	[2.6, 11.1]; 7.4; 7.0
CT3 A&P w	[13.0, 91.0]; 55.4; 58.0	[21.7, 45.0]; 31.1; 30.8	[24.0, 50.5]; 34.0; 33.7	[5.4, 20.0]; 10.4; 9.8
CT3 Chest wo	[24.0, 82.0]; 60.8; 64.0	[23.2, 40.6]; 32.6; 32.6	[11.9, 20.3];15.0; 14.8	[5.9, 24.7]; 12.9; 12.2

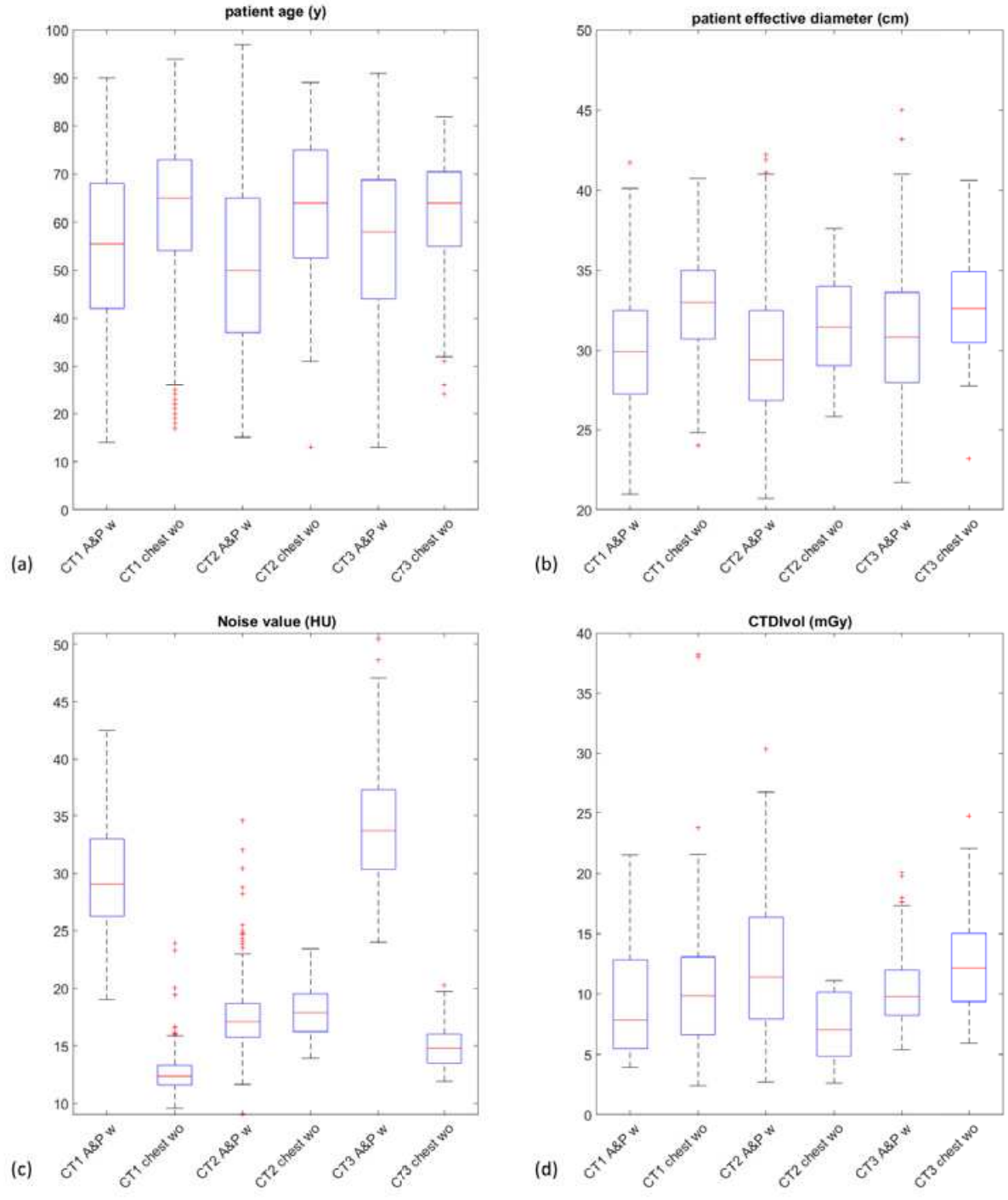

Figure 1. Box plots show median and 25th and 75th percentiles of patient age (a), patient effective diameter (b), noise value (c), and $CTDI_{vol}$ (d) for each scanner model and protocol. Outliers (indicated with + marker) were those that exceeded 1.5 times interquartile length.

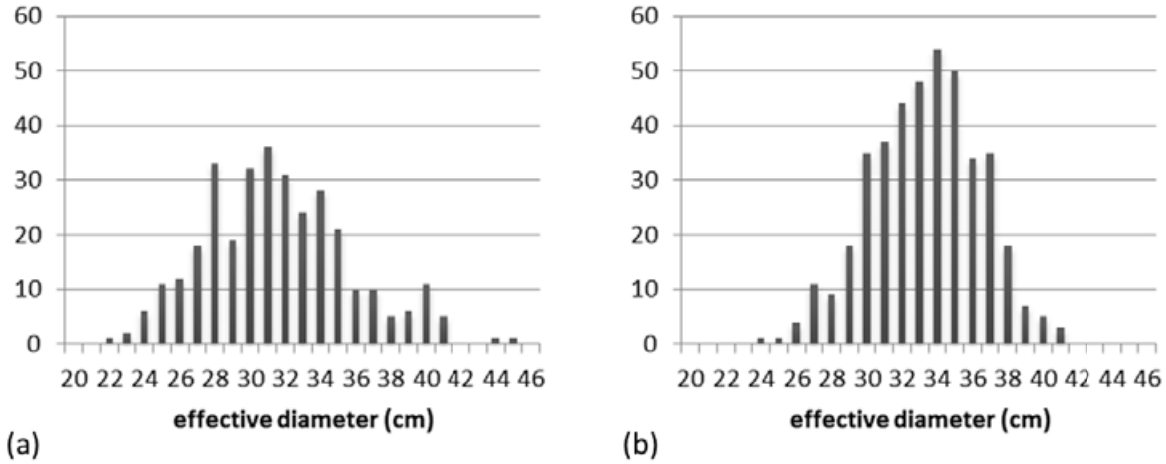

Figure 2. Sample histograms of patient effective diameter. (a) Siemens SOMATOM Definition Flash A&P w protocol. (b) GE Discovery CT750HD Chest wo protocol.

2.B. Description of monitoring program

All data presented in this work came from the Duke Health dose monitoring program (DHDMP). The DHDMP stores patient effective diameter (ED), patient diameter in the anterior-posterior and lateral direction as well as dose and image noise values for all CT studies [8-9]. The patient effective diameter is calculated according AAPM report n.204 [10]. After the CT images are acquired on the scanners, together with the structured dose report, they are sent to both PACS and the Dose Monitoring Server, where images are temporarily stored and then analyzed for patient sizes and noise. The scout images are contoured to calculate the patient sizes, and the tomographic images are used to calculate the noise. The tomographic images are first applied a threshold of -100 ~ 300 HU to isolate soft tissue (relatively uniform and artifact free compared to other tissue types) for noise calculation. For each slice, an ROI (30 pixels × 30 pixels) is identified around each pixel, generating a standard deviation and a histogram of standard deviation map across the slice. Noise of that slice is computed as the value corresponding to the peak of the histogram. The whole CT image set was binned to ten groups and the

noise calculation process is conducted automatically for the first slice for each bin (to reduce the computing time). The final noise value for the image set is computed as the mean of the noise values. A previous study [9] describes in detail this analysis and the reliability of the noise values compared to a phantom and observer analysis. In particular, Christianson et al. have shown that the average absolute difference in noise values were 3.4% in phantom validation and 4.7% in the observer analysis.

2.C. Noise variability

The above method is a sampling of the noise values across the complete slices in one CT study, thus does not address the intrinsic variability of the noise among slices. To estimate this variability, 30 studies (5 abdominopelvic and 5 chest exams for each of the three scanner models) were randomly selected to calculate the noise value in each slice with the same histogram peak value algorithm already implemented in DHDMP. Knowing the noise value for each slice, the standard deviation and the average of the noise value was computed for the complete slices. The percent difference of noise values between the average and the value provided by DHDMP was also computed, namely delta noise. For the 30 studies, the mean of standard deviations were calculated. Similarly for the delta noise, the mean was calculated for the 30 studies.

2.D. Estimation of CT scanner adaptability

To evaluate the scanners' adaptability across a population, dose-patient size dependency and noise-patient size dependency were linearized. For this work, we chose to use the $CTDI_{vol}$ as a dose index as a highly scanner-independent metric. The radiation dose is directly related to the attenuating diameter [8] $CTDI_{vol} \propto e^{d}$, where d is the phantom diameter. Thus $\ln(CTDI_{vol})$ was used as a linear descriptor of $CTDI_{vol}$ as a function of diameter.

In terms of noise, a preceding study [11] reported an empirical equation that relates noise σ, phantom diameter, and tube current (mA) as

$$\ln \sigma = \alpha_0 + \alpha_1 d + \alpha_2 \ln(mA) + \alpha_3 d^2 + \alpha_4 (\ln(mA))^2 + \alpha_5 d \ln(mA), \quad (1)$$

where α_1, α_2, α_3, α_4, α_5 are fitting parameters. Furthermore, an investigation of the ImPACT Group [12] showed a linear proportionality between the logarithm of mA and phantom diameter as

$$\ln(mA) = md + q, \quad (2)$$

where m is the slope, and q is the intercept of the curve. From equations (1) and (2), it follows that

$$\ln \sigma = \alpha_0 + \alpha_1 d + \alpha_2 (md + q) + \alpha_3 d^2 + \alpha_4 (md + q)^2 + \alpha_5 d(md + q). \quad (3)$$

Thus, in a second order approximation, noise can be linearized as a function of patient effective diameter:

$$\sqrt{\ln \sigma} \propto ED. \quad (4)$$

A 3D-fit of $\sqrt{\ln \sigma}$ across $\ln(CTDI_{vol})$ and ED was performed for each protocol and each scanner with a planar 1st degree function. This will characterize the overall dependency of noise versus $CTDI_{vol}$ for each scanner across a population. We used the Curve Fitting Toolbox™ application in MATLAB® R2015b software [13]: in each fit the Root Mean Square Error (RMSE) values were calculated in the residuals' plots as a consistency metric of system adaptability across the study cases.

3. RESULTS

3.A. Noise variability

The intrinsic variabilities of the noise values across the slices in the three scanners involved in this study were calculated for chest and abdominopelvic protocols. The data are shown in Table 3.

Table 3. Values of noise variability (average of the standard deviations of slice-per-slice noise values distribution) and delta noise (mean difference between average noise values in slice-per-slice calculation and the noise values provided by DHDMP) related to the three scanners involved in the study. Values in the brackets are ranges.

Scanner	Protocol	Noise variability (HU)	Delta noise (%)
CT1	A&P w	1.18 [0.40; 2.58]	-0.43 [-2.73; 2.35]
	Chest wo	1.53 [0.84; 1.94]	0.53 [-0.19; 2.45]
CT2	A&P w	3.90 [2.53; 8.96]	1.53 [0.90; 2.51]
	Chest wo	5.91 [3.38; 10.25]	-0.27 [-5.83; 2.58]
CT3	A&P w	2.41 [1.15; 6.08]	0.96 [-1.02; 2.84]
	Chest wo	1.92 [1.18; 3.01]	0.68 [-2.73; 3.27]

3.B. Estimation of CT scanner adaptability

Figure 3 shows the 3D-fit plots of dose versus patient effective diameter with isocontours of noise. The horizontal and vertical axes represent patient diameter and $\ln(CTDI_{vol})$, respectively, while the third axis (color bar) represents the $\sqrt{\ln \sigma}$. The fit was performed with a 1st degree linear function and the RMSE values are summarized in Table 4. Concerning chest exams, $\ln(CTDI_{vol})$ and $\sqrt{\ln \sigma}$ increase with patient diameter for CT2 and CT3, but not for CT1 scanner where the $\sqrt{\ln \sigma}$ decrease with dose and ED. Concerning abdominopelvic exams, the plots show that $\sqrt{\ln \sigma}$ increase only according $\ln(CTDI_{vol})$ for CT1 and CT2, but in CT3 both one and the other increase with patient diameter.

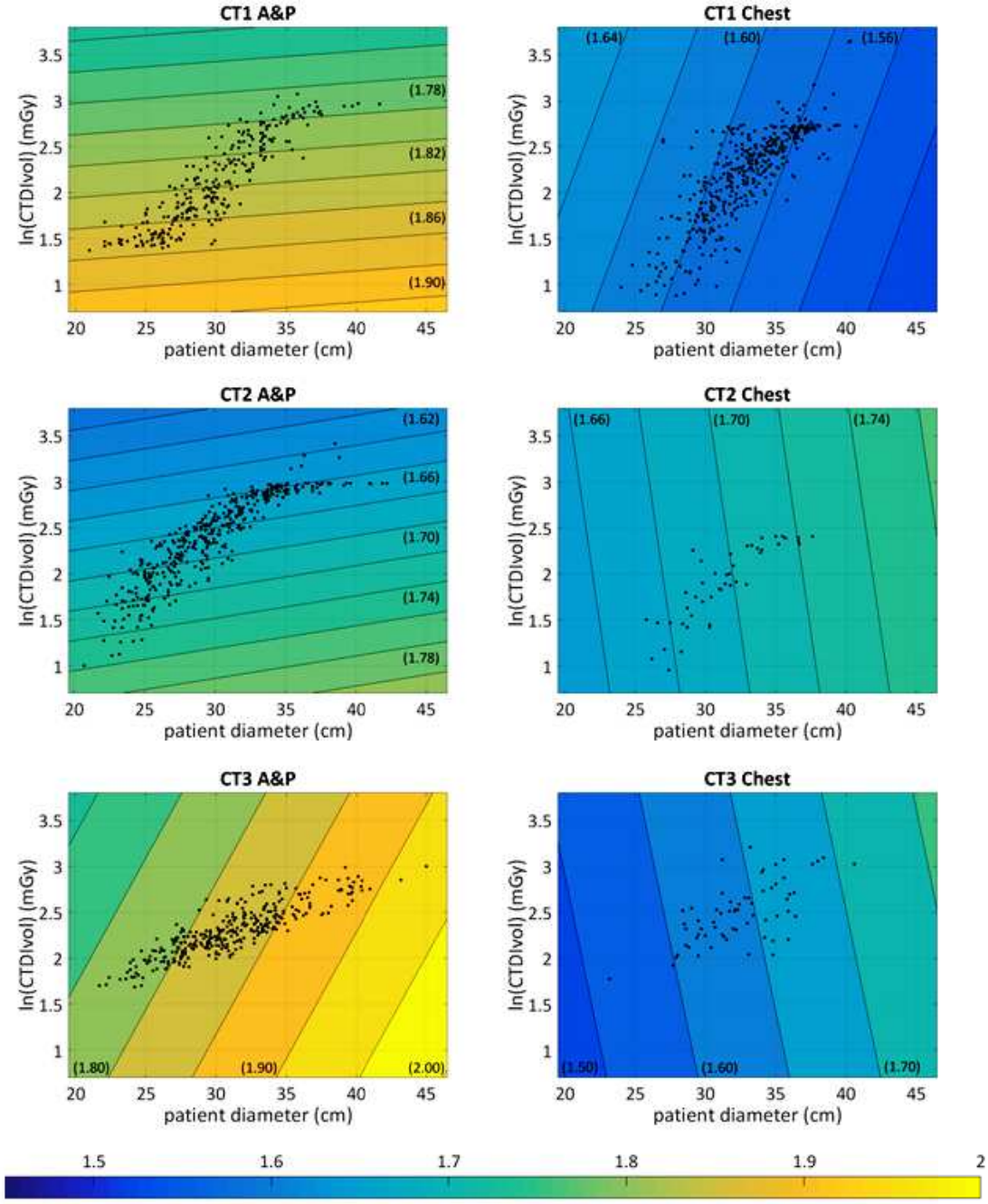

Figure 3. Plots of the 3D fit across the three scanners for A&P w and Chest wo protocols. For each exam (black markers) the color bar represents the noise value information in HU$^{1/2}$ ($\sqrt{\ln \sigma}$, values are within parentheses), the horizontal axis reports patient diameter in cm and the vertical axis represents dose information ($\ln(CTDI_{vol})$) in mGy. From left to right, top to bottom: CT1 A&P, CT1 Chest, CT2 A&P, CT2 Chest, CT3 A&P, CT3 Chest.

Table 4. Summary of RMSE values of the 3D-fit shown in Fig. 2.

Scanner	Protocol	Fit RMSE ($HU^{1/2}$)
CT1	A&P w	0.0344
	Chest wo	0.0344
CT2	A&P w	0.0385
	Chest wo	0.0361
CT3	A&P w	0.0277
	Chest wo	0.0215

4. DISCUSSION

We performed an analysis to compare the performance of different CT scanners with a new metric that simultaneously incorporates image quality information (noise) and radiation dose information ($CTDI_{vol}$) throughout a population of patients. For a given imaging condition, either a fixed mA or ATCM, changes in diameter affects $CTDI_{vol}$. $CTDI_{vol}$ and diameter together result in a noise level in the image. For a given $CTDI_{vol}$, the diameter-noise relationship can be described by the 2D plot. Different $CTDI_{vol}$ values (through changes in the fixed mA value or ATCM settings) would result in different 2D relationship. This 2 way dependency can thus be reflected in a 3D plot that was used in this study. However, although such an analysis could be performed with phantoms, phantom data would only provide information concerning specific exposure parameters for a scan [14]: instead, a general population comparison is a way to obtain new information related to the patient adaptability of different scanners. The analysis was possible by means of the DHDMP, which stores radiation dose information and estimates patient size and noise value data [8-9]. It is possible to reproduce this analysis using patient water equivalent diameter [15] instead that the patient effective diameter estimated by the DHDMP system. To our knowledge, such a comparison across manufacturers that includes dose, noise and patient size information has not been previously reported.

The data show different scanner dependencies in terms of adaptability: the RMSE values for the three scanners are between 0.0385 $HU^{1/2}$ and 0.0215 $HU^{1/2}$. Thus, different scanners offer different degrees of reproducibility of noise and dose values across the population and lower RSME values are associated with better performance reproducibility. In general, for increasing values of dose and patient effective diameter, noise values also increase, with the exception of chest protocol performed with CT1 (for some manufacturer, the ATCM is designed to tolerate more noise for larger patients. Thus, it is possible that image quality decreases even if patient size and dose increase.). Since the study included protocols with different scan parameters and convolution kernels it is not possible to compare the different trends in the 3D plots shown in Figure 2. The study is not affect by the different trends because we have performed the analysis in six populations with consistent scanner parameters and convolution kernels.

Larson *et al.* [7] introduced a mathematical CT radiation dose optimization model based on the minimization of the radiation dose that provides a constant image noise level for different patient sizes. Their model, while innovative and informative, did not consider that the inter-scanner performance and dose administered is not constant across a population. Different scanners have different levels of adaptability. A previous study [9] used the DHDMP algorithm to estimate the variability of noise, SSDE and effective diameter data across the three scanner models involved in this study: the median effective diameter differed by 2-8%, the median SSDE differed by 9-33%, and the median noise values differed by 15-35%, between the three scanner models. In this work, we have shown that the variability cannot be interpreted only in terms of absolute values because scanner performance varies when radiation dose is modulated to achieve consistent image quality across a population.

This study was impacted by an intrinsic variability of the noise data. As noise varies in every slice of CT examinations, the noise value provided by the DHDMP is an average value across the images for a given series of an exam. We estimated the noise variability for every scanner model involved in the analysis as

the average of the SDs of the slice noise populations. Furthermore, we compared the DHDMP data with the average noise value from slice-to-slice calculations. The percentage difference between the two noise estimations was calculated for each scanner and protocol (Table 3) and these variabilities, while embedded in this analysis, are largely comparable across scanners, so they do not invalidate the reported scanners dependencies.

This work is limited in multiple aspects. The work shown here includes only three scanners by two manufacturers and only two different clinical protocols for specific kVp, slice thickness, total collimation width, pitch, image quality indicator and convolution kernel. But, the method described can be implemented to investigate the 3D relationship between noise, radiation dose, and patient size, even for different scan parameters and different image quality indicator values. It should be noted that the results do not show absolute values of image quality and radiation dose across a population but only the difference between different vendors in terms of patient variability. Also, the study does not consider the maximum and minimum tube current values that are set up in certain CT devices. Despite the radiographers can adjust these parameters (i.e. for big patient size), there are not standard clinical procedures that describe the process and this may affect the scanner adaptability. Furthermore, the noise is only one of the parameters that describe image quality in diagnostic imaging, and in future studies, it will be important to investigate the relationship between other image quality indexes (e.g., resolution, contrast) with radiation dose across patient populations, as well as this relationships could be impacted by patient centering in clinical operation. Another limitation is related to the assumption that radiation dose is proportional to e^d. This relationship it has not been proved, conversely Zhou and Boone [16] have shown that radiation dose is not exponentially related to the attenuation diameter for an infinitely long cylinders of water. However, the equation $CTDI_{vol} \propto e^d$ introduces a reasonable model that seems appropriate for the purpose of this work [8].

4.A. Summary

We have shown that it is possible to find a theoretical 3D relationship between image noise, dose ($CTDI_{vol}$), and patient size (effective diameter) in CT examinations. The comparison of real data with this function, in terms of RMSE in a 3D fit, is a metric that describes how different scanners are able to reproduce, for the same patient size, the same performance in terms of an important image quality parameter and in terms of $CTDI_{vol}$. These types of analyses are only possible through simultaneous image quality and dose monitoring, which can speak to the actual (as opposed to presumed) output of imaging systems.

Disclosures of conflicts of interest

The authors have no relevant conflicts of interest related to the present study to disclose.

References

[a)] Author to whom correspondence should be addressed. Electronic mail: francesco.ria@duke.edu

[1] ICRP, 2007d "The 2007 Recommendations of the International Commission on Radiological Protection", ICRP Publication 103, Ann. ICRP **37,** 2–4 (2007).

[2] ICRP, 2007 "Radiological Protection in Medicine" ICRP Publication 105, Ann. ICRP **37**, 6 (2007).

[3] M. Gies, W.A. Kalender, H. Wolf, C. Suess, "Dose reduction in CT by anatomically adapted tube current modulation. Part I. Simulation studies", Medical Physics **26**, 2235-2247 (1999).

[4] W.A. Kalender, H. Wolf, C. Suess, "Dose reduction in CT by anatomically adapted tube current modulation. Part II. Phantom measurements", Medical Physics **26**, 2248-2253 (1999).

[5] M.K. Kalra, M.M. Maher, T.L. Toth, B. Schmidt, B.L. Westerman, H.T. Morgan, and S. Saini, "Techniques and applications of automatic tube current modulation for CT", Radiology **233**, 649-657 (2004).

[6] T.Y. Lee, R.K. Chhem, "Impact of new technologies on dose reduction in CT", European Journal of Radiology **76**, 28-35 (2010).

[7] D.B. Larson, L.L. Wang, D.J. Podberesky, M.J. Goske, "System for verifiable CT radiation dose optimization based on image quality. Part I. Optimization model", Radiology **269** 167-176 (2013).

[8] O. Christianson, X. Li, D. P. Frush, E. Samei, "Automated size-specific CT dose monitoring program: Assessing variability in CT dose", Medical Physics **39**, 7131-7138 (2012).

[9] O. Christianson, J. Winslow, D. P. Frush, E. Samei, "Automated Technique to Measure Noise in Clinical CT Examinations", AJR **205**, W93-W99, 2015.

[10] S. Boone, D. Cody, C. McCollough, M. McNitt-Gray, and T. Toth, "Size specific dose estimates (SSDE) in pediatric and adult body CT examinations," AAPM Report No. 204 (American Association of Physicists in Medicine, College Park, MD, 2011).

[11] X. Li, E. Samei, "Comparison of patient size-based methods for estimating quantum noise in CT images of the lung", Medical Physics **36**, 541-546 (2009).

[12] N. Keat, "Report 05016 CT scanner automatic exposure control systems" ImPACT – London.

[13] "Curve Fitting Toolbox™ User's guide", The MathWorks Inc. Natick, (MA), USA, 2015.

[14] J.J. Sunderland and P.E. Christian, "Quantitative PET/CT scanner performance characterization based upon the Society on Nuclear Medicine and Molecular Imaging Clinical Trials Network Oncology Clinical Simulator Phantom", The Journal of Nuclear Medicine **56**, 154-152 (2015).

[15] AAPM Report no. 220, "Use of Water Equivalent Diameter for calculating patient size and size-specific dose estimates (SSDE) in CT", 2014.

[16] H. Zhou and J. Boone, "Monte Carlo evaluation of $CTDI_{\infty}$ in infinitely long cylinders of water, polyethylene and PMMA with diameters from 10mm to 500mm", Medical Physics **35**, 2424-2431 (2008).